

SpatialReasoner: Towards Explicit and Generalizable 3D Spatial Reasoning

Wufei Ma^{*}, Yu-Cheng Chou^{*}, Qihao Liu^{*}, Xingrui Wang, Celso de Melo[†], Jieneng Chen, Jianwen Xie[°], Alan Yuille

Johns Hopkins University, ^{*}Equal contribution, [†]DEVCOM Army Research Laboratory, [°]Lambda Inc

Recent studies in 3D spatial reasoning explore data-driven approaches and achieve enhanced spatial reasoning performance with reinforcement learning (RL). However, these methods typically perform spatial reasoning in an implicit manner, and it remains underexplored whether the acquired 3D knowledge generalizes to unseen question types at any stage of the training. In this work we introduce SpatialReasoner, a novel large vision-language model (LVLM) that address 3D spatial reasoning with explicit 3D representations shared between stages – 3D perception, computation, and reasoning. Explicit 3D representations provide a coherent interface that supports advanced 3D spatial reasoning and enable us to study the factual errors made by LVLMs. Results show that our SpatialReasoner achieve improved performance on a variety of spatial reasoning benchmarks and generalizes better when evaluating on novel 3D spatial reasoning questions. Our study bridges the 3D parsing capabilities of prior visual foundation models with the powerful reasoning abilities of large language models, opening new directions for 3D spatial reasoning.

Project page (code, models and data): spatial-reasoner.github.io

1. Introduction

3D spatial reasoning studies how models can perceive, understand, and reason about 3D properties of objects and their spatial relationships. It is not only a fundamental task for vision-language models to achieve human-level intelligence, but also crucial to a range of downstream applications in robotics [14, 18] and embodied AI [10]. Recent large vision-language models (LVLMs) explored data-driven approaches to inject 3D knowledge [9, 33] and achieve improved performance on various spatial reasoning benchmarks [31, 46, 52]. On the other hand, large proprietary models such as Gemini 2.0 [15] have advanced 3D parsing by directly predicting 3D object bounding boxes, enabling the development powerful generalist robotics models [44].

Despite recent improvements in thinking models enabled by chain-of-thought reasoning (CoT) [35, 51] and reinforcement learning (RL) [17], state-of-the-art LVLMs continue to struggle with 3D spatial reasoning [31, 52]. We identify two key challenges in 3D spatial reasoning: (1) *3D thinking*—the ability to decompose a complex 3D spatial reasoning question into small, manageable steps, and (2) *3D computation*—the ability to solve these thinking steps in a consistent and accurate manner. As shown in Figure 1, ChatGPT o3 [36] fails to adopt a systematic approach to solving the problem and instead relies on other visual cues to assist the reasoning (e.g., location of the foil package). In contrast, the Gemini 2.0 thinking model [15] employs an organized strategy to tackle the problem but ultimately fails to arrive at the correct answer due to a lack of reliable 3D computation.

In this work, we present SpatialReasoner, a novel large vision-language model (LVLM) with generalizable 3D spatial reasoning from explicit 3D representations. SpatialReasoner builds upon explicit 3D representations as an interface that enable coherent and reliable reasoning across multiple stages, i.e., 3D perception, computation, and reasoning. To achieve this, we adopt a multi-stage training strategy. In Stage I, we apply supervised fine-tuning (SFT) to equip the LVLM with explicit 3D representations, enhancing 3D perception and computation capabilities of the model. Then in

Stage II, we further leverage reinforcement learning (RL) to develop robust and generalizable 3D spatial reasoning built on explicit 3D representations.

We extend the 3D pseudo-annotation pipeline in [33] to synthesize basic 3D perception, *i.e.*, detection and pose estimation, and 3D computation question-answering data interleaved with explicit 3D representations. We further generate standard spatial reasoning question-answer pairs with chain-of-thought reasoning that breaks down complex 3D spatial reasoning questions into multiple steps—3D perception, computation, and reasoning. Experimental results demonstrate that our SpatialReasoner with explicit 3D representations can significantly enhance 3D spatial reasoning abilities of LVLMs and generalize to unseen questions types.

Moreover, we experiment on a range of LVLMs fine-tuned with different combinations of data and training methods to study the key factors towards improved 3D spatial reasoning. Our empirical results lead to the following insights: (1) when developing 3D-aware VLMs, SFT offers a more scalable approach than RL that requires high-quality 3D-aware data that are often difficult to obtain; (2) 3D-aware LVLMs finetuned with RL generalize much better than SFT when tested on novel 3D spatial reasoning questions, echoing prior findings [12]; (3) standard LVLMs often exploit 2D reasoning as a shortcut to tackle 3D spatial reasoning problems, whereas our SpatialReasoner avoids these spurious correlations and always reasons with explicit 3D representations, achieving improved and robust performance on challenging real-world 3D spatial reasoning datasets.

Besides enhancing 3D spatial reasoning capabilities of LVLMs, reasoning with explicit 3D representations allows us to interpret the reasoning process and to study the failure modes of LVLMs. We find that the accuracy of 3D perception lags significantly behind that of 3D reasoning, suggesting that most errors in downstream VQA tasks still stem from failures in 3D perception. Moreover, by predicting key 3D information, such as 3D object locations and orientations, as intermediate results, our SpatialReasoner enables compositional reasoning for 3D spatial tasks [47]. This not only allows our method to generalize better to novel spatial reasoning questions, but also makes it easily extensible to other tasks that build on our explicit 3D representations.

2. Related Works

3D Spatial reasoning. 3D spatial reasoning studies how models can perceive, understand, and reason about 3D properties of objects and their spatial relationships. Early works [47–49] explored this problem in simulation systems extended from CLEVR [20, 24] or existing datasets with object-level 3D annotations [7, 11, 33, 46]. With growing interest in this area, more recent efforts have introduced well-designed 3D spatial reasoning datasets based on real images and videos [31, 52]. To enhance the 3D spatial reasoning capabilities of vision-language models on these benchmarks, prior works adopted data-driven approaches by synthesizing question-answering data on various 3D spatial relationships [9, 11, 33, 39]. Despite their improved performance on downstream benchmarks, these models rely on implicit reasoning and produce final answers directly—without a step-by-step reasoning process or intermediate 3D computation results that we can interpret. Moreover, it remains unclear whether the 3D spatial reasoning capabilities acquired from these data-driven fine-tuning can generalize to novel question types that require complex 3D computation over different combinations of 3D perception outputs.

Explicit 3D representations. Explicit 3D representations can largely simplify the 3D spatial reasoning process and help identify the failure modes of vision-language systems. Previous works often studied this problem in simulation systems using neural-symbolic methods [34]. PO3D [47] exploited compositional 3D vision modules [30] to parse the scene into object-level 3D representations, which

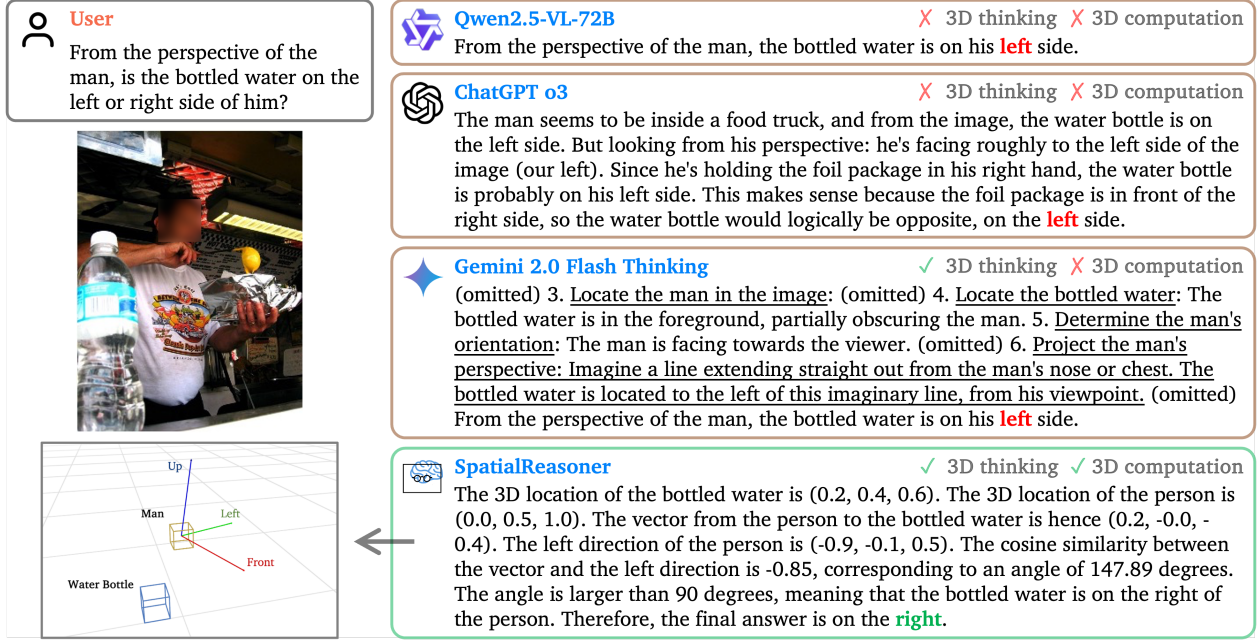


Figure 1 | **Comparing 3D spatial reasoning of our SpatialReasoner with previous state-of-the-art models.** Our SpatialReasoner builds on explicit 3D representations, performs 3D computation, and reasons about the final answer. Although Gemini 2.0 can also break down complex 3D spatial reasoning questions into small and tractable steps, it lacks reliable 3D computation that leads to the correct answer.

are then processed by a neural symbolic reasoner. This method can be further extended to answer temporal questions [48] and spatial relationship questions [49]. These results in simulation systems reveal the limitations of current LLMs and highlight the importance of the visual module for a successful reasoning model.

Post-training. Post-training is a crucial phase that transforms pre-trained language models into task-adaptive and user-aligned systems. While pre-training provides general linguistic and world knowledge, post-training—through techniques such as supervised fine-tuning (SFT), reinforcement learning (RL), and alignment strategies—enables models to follow instructions, incorporate domain expertise, and align with human preferences [21, 45]. Approaches like FLAN [50] and LIMA [55] have demonstrated that SFT improves response formatting and zero-shot performance, while RL methods such as RLHF [5], RLAIF [6], DPO [37], and GRPO [41] further refine model behavior using preference-based feedback and outcome-driven rewards. Together, these strategies have led to models like GPT-4 [1], Claude-3.5 [2], and DeepSeek-R1 [17], showcasing significant advancements in reasoning and alignment. Despite these gains, post-trained models still face challenges in generalization, especially under distribution shifts or novel tasks. Recent studies show that SFT tends to overfit to training patterns, whereas RL enhances reasoning and adaptability through iterative learning and verifier-based rewards [12]. The sequential combination of SFT and RL has proven effective—first stabilizing model outputs, then promoting flexible decision-making [17]. As open-sourced models and instruction datasets continue to expand, post-training remains an active research area critical to building reliable, domain-aware, and ethically aligned LLMs.

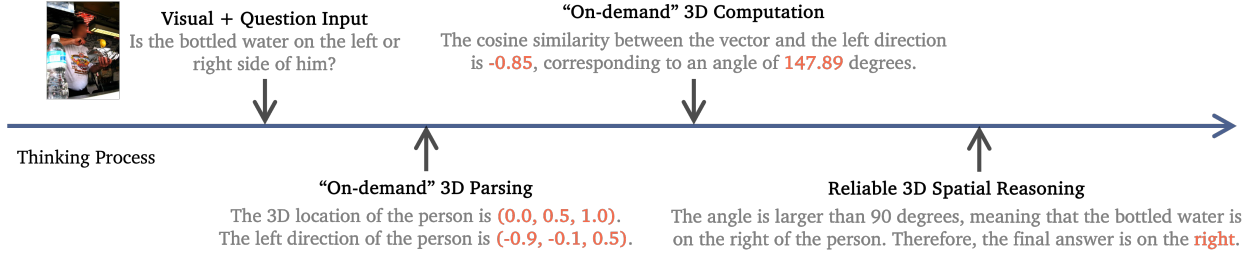


Figure 2 | **Overview of our SpatialReasoner design.** Our SpatialReasoner adopts explicit 3D representations as an interface to enable coherent and reliable multi-stage spatial reasoning, *i.e.*, 3D parsing, computation, and reasoning.

Test-time scaling. Recent advances highlight the importance of test-time scaling, where additional compute and structured reasoning strategies are employed during inference to boost model performance without retraining. Techniques such as beam search [16, 29], best-of-N sampling [43], and Monte Carlo Tree Search (MCTS) [13] enhance output quality by generating multiple candidates and selecting responses based on confidence or self-consistency. Structured prompting methods like Chain-of-Thought (CoT) [51] and Tree-of-Thought (ToT) [54] further improve reasoning by decomposing complex problems into intermediate steps, enabling more interpretable and robust solutions. Beyond decoding strategies, another effective direction involves verifier-guided inference, where models refine outputs iteratively using feedback from trained verifiers [42]. These methods collectively demonstrate that test-time compute, when strategically allocated, serves as a powerful tool for enhancing reasoning in both unimodal and multimodal models. Our work extends these findings by applying CoT reasoning in the context of 3D spatial understanding. Specifically, we fine-tune models to generate step-by-step reasoning traces that capture perceptual, computational, and inferential processes in 3D tasks. By explicitly modeling intermediate rationales, CoT fine-tuning enhances both interpretability and performance on complex spatial reasoning benchmarks.

3. SpatialReasoner

3.1. Overview

In this section, we introduce our SpatialReasoner for explicit and generalizable 3D spatial reasoning. Our SpatialReasoner features two key designs: (1) explicit 3D representations that serves as interface to support multi-stage spatial reasoning, *i.e.*, 3D parsing, computation, and reasoning (see Figure 2), and (2) generalizable spatial reasoning from multi-stage training (see Figure 4).

In Section 3.2, we present the explicit 3D representations and describe how our model is trained to predict and to interpret the 3D representations for spatial reasoning. Then in Section 3.3 we discuss our training strategies, exploring standard supervised fine-tuning, reinforcement learning, as well as 3D-aware process rewards. Lastly we introduce our 3D-aware data generation pipeline and different variants of training data used at different stages in Section 3.4.

3.2. Learning Explicit 3D Representations

Despite the improved spatial reasoning abilities achieved by 3D-aware LVLMs, such as SpatialRGPT [11] and SpatialLLM [33], and advanced proprietary models like Gemini 2.0 [15], these methods lack explicit 3D representations and instead rely on natural language to perform 3D spatial reasoning. For example, Gemini 2.0 predicts 3D object poses with descriptions like “facing towards the viewer and

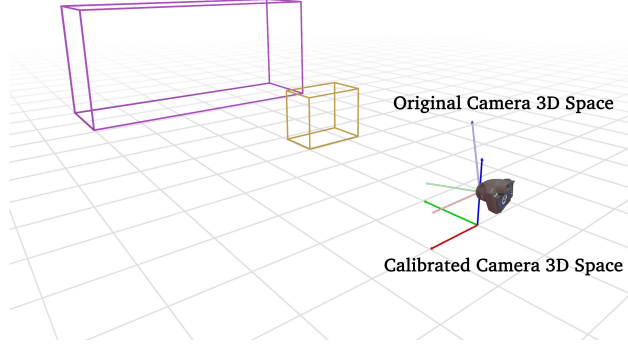


Figure 3 | **Comparison between original and calibrated camera 3D space.** Our explicit 3D representations are defined within calibrated camera 3D space that simplifies subsequent 3D computations.

slightly to its right” and estimate 3D distances with phrases such as “far behind some other object”. These natural language descriptions are inefficient and often not accurate enough for complex 3D spatial reasoning.

Therefore, we propose to integrate LVLMs with explicit 3D representations, such as 3D locations and poses, to serve as an accurate and reliable interface shared across multiple stages of 3D spatial reasoning (see Figure 2). Our SpatialReasoner can either predict (output) explicit 3D representations as intermediate results or take them as inputs to perform basic 3D computations or complex spatial reasoning tasks.

Explicit 3D representations. We define explicit 3D representations in a calibrated camera 3D space, which is a standard camera 3D space calibrated with extrinsics of the camera. As illustrated in Figure 3, the calibrated camera 3D space has its z -axis aligned with the z -axis of the 3D world space, and the origin on the z -axis is positioned close to the ground plane. Although estimating 3D object locations tends to be easier in original camera 3D space, adopting explicit 3D representations in calibrated camera 3D space offers many advantages for subsequent spatial reasoning: (1) the z -coordinates directly correspond to object heights, (2) estimating 3D spatial relationships such as “above” and “below” are largely simplified, and (3) objects often are on a plane parallel to the ground plane, which reduces many 3D spatial relationships to simpler 2D problems.

A unified interface for explicit 3D spatial reasoning. Explicit 3D representations serve as an interface that enables coherent and accurate 3D spatial reasoning across multiple stages (see Figure 2). For 3D perception, the model predicts object locations and orientations as 3D vectors. It then estimates explicit distances or angles based on these predictions. Lastly, the model aggregates explicit 3D information from previous stages to reason about and answer various 3D spatial reasoning questions.

3.3. Training Strategies

Supervised fine-tuning (SFT). We adopt a two-stage post-training strategy to equip the model with explicit and generalizable 3D spatial reasoning capabilities. In the first stage, SFT serves as a critical initialization step, aligning the pre-trained LVLM with curated the 3D-annotated datasets. By optimizing a maximum likelihood objective over paired input-output sequences, the model learns to parse 3D scenes and predict explicit representations such as object locations and orientations. This structured supervision enables the model to expose interpretable intermediate reasoning traces during

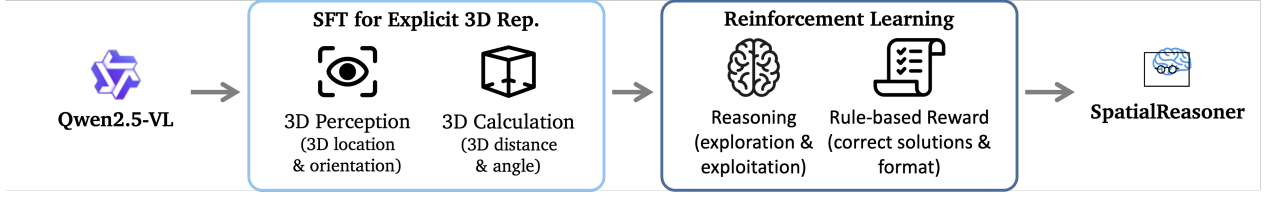


Figure 4 | **Overview of our SpatialReasoner training.** We adopt a multi-stage training strategy: In Stage I, we apply supervised fine-tuning (SFT) to equip the LVLM with explicit 3D representations; then in Stage II, we leverage reinforcement learning (RL) to develop robust and generalizable 3D spatial reasoning built on explicit 3D representations.

spatial computations—e.g., calculating relative distances and angle. However, due to its reliance on static demonstrations, SFT exhibits limited capacity to generalize beyond observed reasoning patterns. As demonstrated in Section 4.3, SFT-trained models tend to memorize spatial templates in the training set and struggle with novel compositions or combinatorial variations in 3D queries.

Reinforcement learning (RL). To overcome this limitation, we further post-train the SFT-initialized model using reinforcement learning (RL) with rule-based rewards. Treating the spatial reasoning task as a sequential decision process, each reasoning step is framed as an action within a Markov Decision Process (MDP), and policy gradients are optimized using GRPO [41]. Importantly, we integrate a reward scheme that provides structured reward signals reflecting both the correctness of final answers and the coherence of intermediate 3D computation steps. This enables multi-turn optimization where the model learns to revise inaccurate inferences and explore alternative reasoning paths. Empirically, this RL stage substantially improves generalization to out-of-distribution 3D spatial questions (Table 3), particularly in settings involving novel object arrangements or ambiguous geometric configurations. The combined SFT+RL strategy therefore balances response formatting and perceptual grounding with adaptive reasoning and robustness, making it especially suited for complex 3D spatial understanding.

Reward and policy optimization design. To effectively train our SpatialReasoner via reinforcement learning, we design a composite reward scheme that reflects both the correctness of final predictions and the quality of intermediate reasoning processes. For outcome reward modeling, we employ two components: an accuracy reward and a format reward. The accuracy reward is a rule-based binary signal that aligns with the multiple-choice evaluation metric from MMBench [27], assigning positive feedback only if the predicted answer matches the ground-truth label. Complementing this, the format reward—adopted from DeepSeek-R1 [17]—encourages well-structured answers, promoting output consistency and readability.

Beyond final answer correctness, we explore process reward modeling to examine whether the model can independently learn desirable reasoning trajectories without relying on SFT. The reasoning steps reward provides positive feedback when responses include structured indicators such as “First”, “Second”, “Next”, and “Therefore” which enhance the fluency and interpretability of multi-step inference. The 3D-aware process reward, tailored per question type, evaluates whether necessary 3D perception or calculation terms are present in the reasoning process, such as references to distance, location, or orientation estimation. The reward signal is then calculated through the accuracy of presence of each terms. Although these two process rewards are not used in the final model, they provide a valuable diagnostic tool for examining whether LLMs can self-organize into plausible 3D reasoning trajectories without relying on SFT.

Lastly, we ablate the impact of the KL divergence constraint in GRPO and observe that its inclusion leads to degraded training accuracy despite stabilizing output lengths (Section 4.3). Consequently, we remove the KL term to improve alignment with correct spatial answers.

3.4. Training Data

To enable LVLMs to predict and reason with explicit 3D representations and to post-train LVLMs to solve various challenging 3D spatial reasoning questions, we generate a series of 3D-aware training data. We extend the data generation pipeline in [9, 11, 33]. Our process begins with generating 3D pseudo-annotations, followed by optional human verification, and ends with constructing various VQAs and chain-of-thought reasoning based on the 3D pseudo-annotations.

Pseudo 3D ground-truths. We extend the 3D pseudo-annotation pipeline proposed in [9, 33] and generate various 3D annotations, such as object category, 3D location, and 3D pose, on unlabeled images from the OpenImages dataset [22]. Based on the object-level 3D annotations, we then apply rule-based methods to derive ground-truth labels for a range of 3D spatial relationships. Despite significant progress in visual foundation models for segmentation [38], metric depth estimation [53], and object pose estimation [32], we notice many factual errors in the generated 3D ground-truth, particularly when mistakes (e.g., missing objects or inaccurate object poses) propagate through the data pipeline. Therefore, we adopt a series of aggressive filtering steps to ensure the quality of our training data, including: (1) removing images with densely cluttered scenes, (2) excluding object categories that are difficult to segment or estimate pose for, and (3) discarding boundary cases that could lead to ambiguity.

Human verification. Despite leveraging state-of-the-art visual foundation models in our data generation pipeline and applying multiple filtering strategies, we notice that the 3D pseudo-annotations remain susceptible to factual errors. Specifically, small errors such as missing objects or inaccurate 3D pose predictions are propagated to later stages of the data pipeline, leading to various factual errors in the final spatial relationship pseudo-annotations. To investigate the impact of data quality, we create a smaller but higher-quality dataset by manually verifying the correctness of the 3D pseudo-annotations.

Training data variants. Based on the obtained 3D ground-truth, we can generate different variants of data for fine-tuning. Specifically, we consider the following: (1) *Basic3D-QA* consists of basic 3D perception and 3D computation question-answering data. This can be used to learn explicit 3D representations without training on various 3D spatial relationships considered in downstream tasks. (2) *SR-QA* contains visual question-answering pairs about various 3D spatial relationships, following previous 3D-aware datasets [11, 33]. (3) *SR-Cot* extends SR-QA and comprises chain-of-thought reasoning with explicit 3D representations. Questions are answered in a step-by-step manner.

4. Results

4.1. Experimental Setup

Baselines. We compare our SpatialReasoner with the following three types of baseline models. (1) *Open-sourced generalist models*: such as LLaVA [26], Cambrian-1 [46], and Qwen2.5 [4] that are trained on general vision-language data. (2) *Open-sourced specialist models*: We evaluate SpaceLLaVA [40], which is a public re-implementation of SpatialVLM [9], SpatialBot [8] that enhances fine-grained spatial reasoning and robot control by utilizing both RGB and depth images, and

Method	Mean	Height	Location	Orientation	Multi-Object
Open-Sourced Generalist					
LLaVA-v1.5-7B [26]	38.1	39.1	46.9	28.7	34.7
Cambrian-1-8B [46]	42.2	23.2	53.9	35.9	41.9
Qwen2.5-VL-7B-Instruct [4]	48.4	44.1	62.7	40.6	40.5
Open-Sourced Specialist					
SpaceLLaVA [40]	42.0	49.3	54.4	27.6	35.4
SpatialBot [8]	41.0	40.4	54.4	31.9	33.5
SpatialLLM [33]	44.8	45.8	61.6	30.0	36.7
Proprietary					
GPT-4o-mini	39.7	44.3	52.4	21.0	36.5
GPT-4o	44.2	53.2	59.6	21.6	39.0
Claude 3.5 V Sonnet	48.2	53.5	63.1	31.4	41.3
Gemini 2.0 Flash	49.8	49.7	68.9	32.2	41.5
Gemini 2.0 Flash (thinking)	51.1	53.0	67.1	35.8	43.6
Ours					
SpatialReasoner-Zero	54.0	46.4	67.3	48.4	47.2
SpatialReasoner-SFT	<u>58.3</u>	51.9	<u>73.5</u>	<u>50.7</u>	<u>50.3</u>
SpatialReasoner	60.3	<u>52.5</u>	75.2	55.2	51.8

Table 1 | **Comparison with previous state-of-the-art methods on 3DSRBench [31].** Our SpatialReasoner outperforms previous open-source and proprietary methods on challenging 3D spatial reasoning problems in 3DSRBench [31].

SpatialLLM [33] that finetunes a LLaVA model with multi-stage 3D-informed training. Note for fair comparison, we evaluate SpatialBot with RGB inputs only. (3) *Proprietary models* such as GPT-4o [1] and Claude 3.5 [3] that have been trained on abundant web-scale data and for Gemini 2.0 [15], additional 3D-aware post-training.

Evaluation benchmarks. We evaluate spatial reasoning abilities of various models on three spatial reasoning benchmarks. *3DSRBench* [31] is a comprehensive 3D spatial reasoning benchmark with 2,100 questions and studies various 3D awareness and reasoning abilities with a robust evaluation setup. *CVBench* [46] is a vision-centric benchmark that assess models at classic vision tasks with a range of 2D and 3D understanding VQAs. In this work, we focus exclusively on 3D-related questions, *i.e.*, CVBench-3D, as 2D left-right relationships can lead to ambiguity with 3D left-right questions considered in 3DSRBench. *GQA* [19] is a widely adopted benchmark that studies visual reasoning and compositional question answering on a range of spatial relationships between objects.

4.2. Advancing 3D Spatial Reasoning

We evaluate SpatialReasoner across 3DSRBench [31], CVBench-3D [46], and GQA [19] to systematically assess 3D perception, computation, and reasoning capabilities. As shown in Table 1, SpatialReasoner achieves a new state-of-the-art mean accuracy of 60.3% on 3DSRBench, substantially outperforming prior open-source and proprietary models. Compared to Gemini 2.0 Flash (49.8%) and Claude 3.5 Sonnet (48.2%), our model demonstrates significant gains across all dimensions, with particularly strong improvements in Location (+6.3%) and Orientation (+14.6%) questions relative to the second-best model, reflecting better 3D perception and computation abilities. Furthermore, SpatialReasoner attains 51.8% (+8.2%) accuracy on Multi-Object questions, highlighting its ability to reason about complex spatial interactions involving multiple entities.

On depth-related questions in CVBench-3D and GQA (see Table 2), SpatialReasoner maintains

Method	CV-Bench-3D			GQA					
	Mean	Depth	Distance	Mean	Choose	Compare	Logical	Query	Verify
Qwen2.5-VL-7B-Instruct [4]	82.8	82.5	83.2	58.8	82.7	71.5	78.9	40.6	82.5
SpatialReasoner-Zero	79.7	77.5	<u>81.8</u>	60.2	81.6	67.9	<u>79.2</u>	43.8	82.1
SpatialReasoner-SFT	78.3	<u>85.2</u>	71.5	62.0	<u>82.8</u>	<u>72.2</u>	81.4	45.5	83.2
SpatialReasoner	<u>80.3</u>	87.3	73.3	<u>61.8</u>	83.2	81.1	71.8	<u>45.2</u>	<u>82.9</u>

Table 2 | **Performance on CV-Bench-3D and GQA.** Our SpatialReasoner also improves the spatial reasoning performance on GQA [19] and depth-related questions in CVBench-3D [46]. Regarding the performance on distance-related questions in CVBench-3D, see Section 4.2 and Section B for detailed discussions.

Method	Mean	Height	Location	Orientation	Multi-Object
Qwen2.5-VL-7B-Instruct [4]	48.4	44.1	62.7	40.6	40.5
SpatialReasoner-Zero	<u>53.7</u>	40.6	68.4	<u>50.2</u>	46.6
SpatialReasoner-SFT	52.2	<u>44.9</u>	<u>69.5</u>	48.9	40.0
SpatialReasoner	56.4	<u>52.5</u>	<u>72.6</u>	54.1	<u>43.4</u>

Table 3 | **Evaluation of novel question types by withholding multi-object reasoning questions during training.**

strong generalization, achieving a mean accuracy of 80.3% on CVBench-3D and excelling particularly in depth-related spatial perception with an 87.3% score. In GQA, our model shows improved performance in the Compare category, further supporting enhanced multi-object reasoning capabilities. These improvements validate the strength of our multi-stage training pipeline: SFT grounds the model with explicit 3D representations for accurate perception and basic spatial computations, while RL promotes adaptive multi-step reasoning and generalization to novel 3D spatial configurations. Collectively, these advances establish SpatialReasoner as a new benchmark for vision-language models in 3D spatial reasoning tasks.

However, we observe a noticeable drop in the performance of SpatialReasoner on distance-related questions in CVBench-3D. This stands in contrast to the significant improvement performance on similar questions in 3DSRBench (“multi-object-closer-to”), where performance increases from 34.3% to 70.9%. We attribute this discrepancy to the abundant shortcuts present in distance-related questions in CVBench-3D, where LVLMs tend to exploit 2D spurious correlations as a shortcut for 3D spatial reasoning. In contrast, our SpatialReasoner builds on explicit 3D representations, enabling it to better tackle challenging real-world 3D spatial reasoning questions. Please refer to Section B for detailed discussions.

4.3. Analyses and Findings

Generalization abilities. Recent studies have shown that while SFT helps stabilize model outputs, it tends to cause memorization, limiting generalization, especially when encountering out-of-distribution (OOD) variations [12]. In contrast, RL, particularly when using outcome-based rewards, enhances a model’s ability to learn transferable principles, enabling better adaptation to unseen tasks and improving perceptual capabilities. Motivated by these findings, we design an experiment to assess how different post-training strategies—SFT, RL, and their combination—affect generalization in spatial reasoning, specifically on multi-object scenes, which are often more challenging due to increased visual and relational complexity.

To evaluate this, we removed all multi-object training data and trained three models: SpatialReasoner-

Method	Mean
Qwen2.5-VL-7B-Instruct [4]	48.4
SpatialReasoner-SFT	58.3
SpatialReasoner-SFT (w/o explicit 3D rep.)	51.9

Table 4 | **Comparisons between SpatialReasoner without explicit 3D representations and chain-of-thought reasoning.**

Method	Mean
Qwen2.5-VL-7B-Instruct [4]	48.4
SpatialReasoner-SFT	58.3
SpatialReasoner-SFT (+HQ SFT)	54.7
SpatialReasoner-Zero	54.0
SpatialReasoner-Zero (w/ KL)	52.4
SpatialReasoner-Zero (w/ 3D Rwd)	54.6

Table 5 | **Comparisons between design choices in RL and SFT.**

Zero (RL-only), SpatialReasoner-SFT (SFT-only), and SpatialReasoner (SFT+RL). As shown in Table 3, the multi-object performance of SpatialReasoner-Zero (46.6%) substantially surpasses that of SpatialReasoner-SFT (40.0%), highlighting that RL training alone provides better zero-shot generalization to multi-object reasoning tasks than SFT alone. Furthermore, combining SFT and RL (SpatialReasoner, 43.4%) further improves over SFT, but does not fully match the RL-only model’s multi-object performance when trained without direct supervision. This trend echoes the hypothesis that SFT tends to overfit to the specific distributions seen during training, while RL promotes more flexible reasoning capabilities.

When multi-object training examples exist (Table 1), SFT can simply memorize the structure and examples of multi-object scenes through direct supervision, resulting in reasonable performance by relying on pattern matching (50.3% vs. 40.5%). However, when multi-object examples are removed, SFT performance drops sharply (40.0% vs. 50.3%), while RL-tuned models continue to generalize well (46.6% vs. 47.2%). This suggests that RL is not merely memorizing the training-specific distributions but is instead internalizing transferable and compositional reasoning capabilities, enabling robust generalization to complex unseen multi-object scenarios.

Beyond the multi-object class performance, we also analyze the overall mean performance changes across settings. As shown in Table 1 and Table 3, SpatialReasoner-Zero maintains almost the same mean performance (54.0% vs. 53.7%), indicating that RL training enables strong generalization even when multi-object examples are removed. In contrast, SpatialReasoner-SFT suffers a substantial mean performance degradation (58.3% vs. 52.2%), reflecting its reliance on memorizing specific training distributions. Overall, these results reinforce the conclusion that outcome-based RL training enables models to acquire more robust and transferable reasoning capabilities, while SFT alone remains vulnerable to overfitting to seen distributions.



While SFT helps stabilize outputs, it tends to overfit training distributions, whereas outcome-based RL encourages the development of transferable reasoning strategies that enable robust generalization to unseen scenarios.

Scaling of training computation. We ablate on the scaling of training computation for SpatialReasoner-SFT and SpatialReasoner in Figure 5. Results show that with more training steps, SpatialReasoner-SFT starts to overfit and exhibit decreased performance, while SpatialReasoner trained with RL retains a stable and competitive performance.

Scaling of training data. A major challenge for 3D-related tasks is the availability of high-quality data with 3D (pseudo-)annotations. Since annotating 3D data is often time-consuming and requires

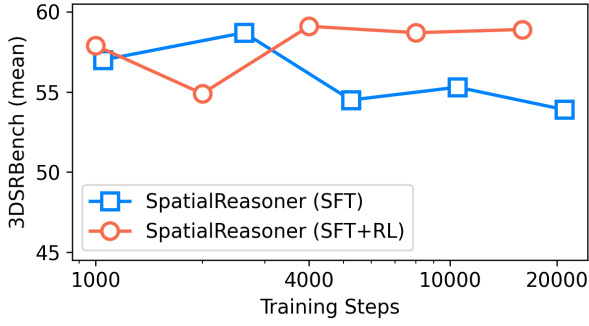


Figure 5 | **Scaling of training computation (in number of epochs).**

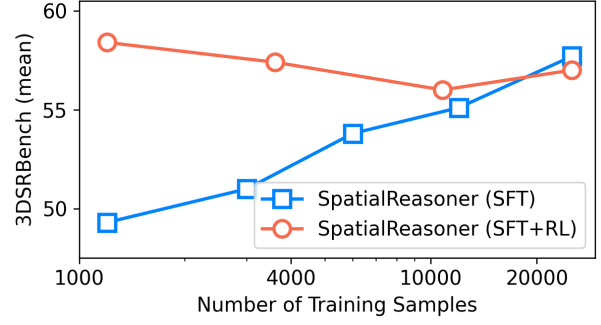


Figure 6 | **Scaling of training data by mixing 1.2K human verified data with 24K unverified data.**

certain expertise, real-world images with accurate 3D annotations are often limited in quantity. On the other hand, synthetic data with 3D ground-truths or real-world images with automated pseudo-annotations are more abundant in quantity, but they inevitably introduce challenges such as domain gaps and noisy supervision.

To study the data scaling properties of our SpatialReasoner with or without reinforcement learning, we experiment on a range of training data sizes by mixing 1.2K human verified 3D data with 24K unverified 3D data. We visualize the data scaling results in Figure 6 and find that SpatialReasoner trained with RL achieves the best performance when only 1.2K human verified data is used, which is in contrast to SpatialReasoner-SFT that scales effectively with the availability of more unverified 3D data. This shows that SFT is more robust to noisy pseudo-annotations and benefits from data scaling, while fewer but higher-quality data are desirable for RL.



When developing 3D-aware LLMs, SFT offers a more scalable approach given the availability of abundant, albeit possibly noisy, 3D pseudo-annotations, whereas RL benefits more from high-quality 3D data that are often limited in quantity.

Ablation study on process reward modeling. We conduct an ablation study to assess whether explicit 3D reasoning trajectory can emerge purely from process reward modeling, without relying on costly curated chain-of-thought supervision. Through qualitative analysis (Figure 7), we observe that SpatialReasoner-Zero trained with 3D-aware process rewards can independently generate structured multi-step reasoning, correctly grounding its inferences through 3D locations, orientation estimation, and relational comparisons—despite not being exposed to manually crafted reasoning examples. Compared to SpatialReasoner-Zero, which often produces shortcut answers without sufficient process grounding, the enhanced model demonstrates a clear improvement in interpretability and reasoning fluency. Quantitatively, as shown in Table 5, incorporating 3D-aware process rewards leads to a performance increase from 54.0% to 54.6%, highlighting that outcome-driven reward shaping can foster coherent reasoning without relying on costly human-curated chains of thought. For the final SpatialReasoner model, however, we rely on SFT to establish desirable reasoning processes, given its superior performance compared to process reward modeling alone.



Without abundant high-quality CoT reasoning data for SFT, our process reward modeling can effectively induce interpretable multi-step reasoning trajectories and enhance model performance.



User

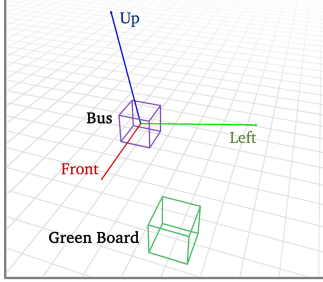
Consider the real-world 3D locations and orientations of the objects. Which side of the bus is facing the green board? A. right, B. front, C. left, D. back.

SpatialReasoner-SFT w/o explicit 3D representation

D. back.

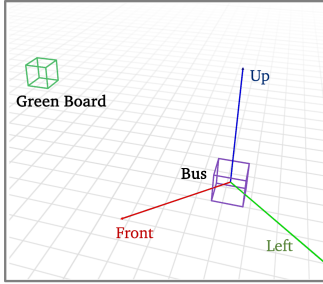
SpatialReasoner-Zero

<think>The green board is on the front of the bus.</think><answer>B.</answer>



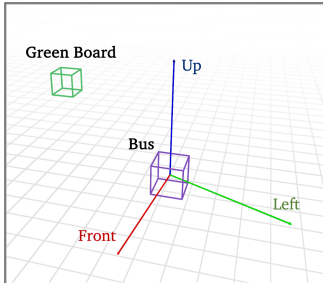
SpatialReasoner-Zero w/ 3D-aware process reward

<think>First, I will determine the front direction of the bus. The front direction of the bus is $(-0.17, 0.25, -0.96)$. Next, I will calculate the 3D location of the bus and the green board. The 3D location of the bus is $(3.97, 2.35, 17.15)$, and the 3D location of the green board is $(1.75, 1.65, 13.95)$. Then, I will calculate the vector from the bus to the green board. The vector is $(-1.70, 0.00, 0.99)$. After that, I will determine the left direction of the bus. The left direction of the bus is $(-0.92, 0.37, -0.29)$. Finally, I will check the angle between the front direction and the green board and compare it with the angle between the left direction and the green board. The angle between the front direction and the green board is 0.29 and the angle between the left direction and the green board is 0.33. Therefore, the correct answer is the front side of the bus facing the green board.</think><answer>B. front</answer>



SpatialReasoner-SFT

The 3D location of the bus is $(-4.3, 1.9, 17.7)$. The 3D location of the green board is $(4.9, 2.9, 22.1)$. The vector from the bus to the green board is hence $(9.2, 0.9, 4.4)$. The left direction of the bus is $(-0.7, 0.0, -0.7)$. The cosine similarity between the vector pointing to the green board and the left direction is -0.94 , corresponding to an angle of 160.87 degrees. Thus the angle between the vector pointing to the green board and the right direction is 19.13 degrees. The front direction of the bus is $(0.7, 0.0, -0.7)$. The cosine similarity between the vector pointing to the green board and the front direction is 0.34, corresponding to an angle of 70.30 degrees. Thus the angle between the vector pointing to the green board and the back direction is 109.70 degrees. Among the four directions, the smallest angle is right direction, with an angle of 19.13 degrees. Thus right side of the bus is facing the green board. Therefore, the final answer is A. right.



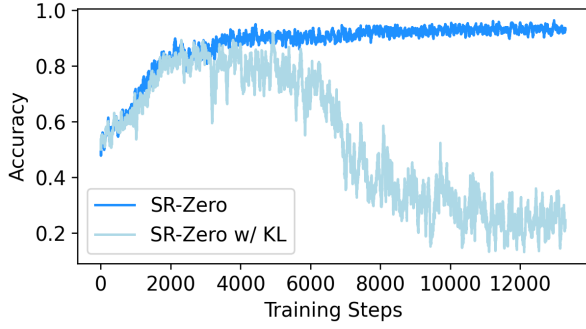
SpatialReasoner

<think>The 3D location of the bus is $(-3.7, 2.1, 14.7)$. The 3D location of the green board is $(2.2, 3.1, 19.8)$. The vector from the bus to the green board is hence $(5.9, 1.0, 5.1)$. The left direction of the bus is $(-0.9, 0.0, -0.4)$. The cosine of the angle between the vector pointing to the green board and the left direction is -0.99 , corresponding to an angle of 172.09 degrees. Thus the angle between the vector pointing to the green board and the right direction is 7.91 degrees. The front direction of the bus is $(0.1, 0.0, -1.0)$. The cosine of the angle between the vector pointing to the green board and the front direction is -0.15 , corresponding to an angle of 98.47 degrees. Thus the angle between the vector pointing to the green board and the back direction is 81.53 degrees. Among the four angles, the smallest is the right direction (7.91 degrees), which is the answer to this question.</think><answer>right</answer>

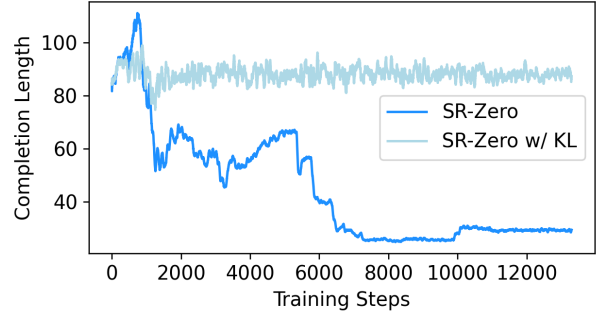
Figure 7 | Qualitative results.

Ablation study on explicit 3D representations. To study the importance of explicit 3D representations and step-by-step 3D computations, we train a variant of SpatialReasoner on the same data but without explicit 3D representations. Results in Table 4 show that explicit 3D representations can enhance 3D spatial reasoning by a wide margin.

Ablation study on KL divergence. We investigate the role of KL divergence regularization in GRPO and find that, although it traditionally serves to constrain policy drift and maintain linguistic stability during reward optimization, it significantly impairs learning in our setting. As shown in Figure 8, adding a KL constraint leads to an eventual collapse in training accuracy, while the model trained without KL divergence achieves stable improvements, reaching nearly perfect accuracy. Compared to the stable completion length under KL regularization, the reduced completion length without KL



(a) Accuracy of SpatialReasoner-Zero w/ and w/o KL divergence.



(b) Completion length of SpatialReasoner-Zero w/ and w/o KL divergence.

Figure 8 | **Training curve between SpatialReasoner-Zero and SpatialReasoner-Zero w/ KL.**

might arise from mitigated length bias [28], indicating improved token efficiency. Quantitatively, as summarized in Table 5, SpatialReasoner-Zero achieves a higher accuracy of 54.0% compared to 52.4% when KL divergence is included. Based on these observations, we remove the KL divergence term from GRPO to promote better alignment with correct spatial reasoning answers.

Ablation Study on SFT+RL vs. SFT+SFT To isolate the effect of RL and verify that performance gains are not merely from additional data exposure, we compare sequential SFT+RL against SFT+SFT. As shown in Table 5, while SpatialReasoner-SFT achieves 58.3% accuracy, applying a second round of SFT (SFT+SFT) degrades performance to 54.7%. In contrast, switching to RL after SFT (SFT+RL) improves accuracy to 60.3%. These results indicate that repeated SFT exacerbates overfitting to training patterns, whereas RL effectively builds on the structured outputs from SFT to promote more adaptive and generalizable 3D spatial reasoning.

4.4. Interpreting Failure Modes

Explicit 3D representations not only enhance 3D spatial reasoning, but also improve the interpretability of vision language systems [47]. We broadly categorize the 3D spatial reasoning into two stages: 3D perception, which parses crucial 3D information from the image input, and 3D reasoning, which computes key 3D metrics and derives the final answer.

To quantitatively study how models behave in the two stages, we manually evaluate the 3D pseudo-annotations generated by our data pipeline and obtain a total of 300 questions with human verified 3D answers. For 3D perception, we consider two types of questions that consider the 3D location and 3D orientation of the object. For 3D reasoning, models need to estimate distances, depths, and angles given 3D information such as locations and directions. Specifically, angles and directions are evaluated with prediction accuracy with a threshold of $\pi/6$ (30 degrees), while locations and distances are evaluated with mean error.

From the results in Table 6, we observe that 3D reasoning can estimate angles, distances, and depths a lot more accurate than 3D perception that predicts orientations and locations from visual features. This observation aligns with findings from the qualitative examples where we visualize the predictions in a simulation system. We conclude that the majority of the errors made in downstream VQA tasks still stem from errors in 3D perception. Moreover, RL slightly hurts the accuracies of 3D perception and reasoning. This is because the RL rewards only consider the format of the reasoning or the correctness of the final answer, ignoring all intermediate explicit 3D representations.

Method	3D Perception		3D Reasoning		
	Orientation (\uparrow)	Location (\downarrow)	Angle (\uparrow)	Distance (\downarrow)	Depth (\downarrow)
SpatialReasoner-SFT	35.5	0.91	55.0	0.17	0.13
SpatialReasoner	31.0	1.05	52.5	0.19	0.25

Table 6 | **Studying failure modes of SpatialReasoner.** We observe that 3D reasoning can estimate angles, distances, and depths a lot more accurate than 3D perception that predicts orientations and locations from visual features.

5. Conclusions

In this paper, we introduced SpatialReasoner, a novel large vision-language model (LVLM) that performs explicit and generalizable 3D spatial reasoning by predicting and leveraging intermediate 3D representations across perception, computation, and reasoning stages. Through a two-stage post-training pipeline combining supervised fine-tuning and reinforcement learning, our method significantly advances the spatial reasoning abilities of LVLMs, achieving new state-of-the-art results across multiple benchmarks while maintaining strong generalization to novel 3D reasoning tasks. By systematically analyzing model behaviors, we demonstrate that reasoning grounded in explicit 3D representations not only improves accuracy but also offers interpretable reasoning traces and highlights critical bottlenecks in 3D perception. Our study underscores the importance of structured reasoning and adaptive training strategies for robust 3D understanding, opening new opportunities for future research at the intersection of visual perception, geometric computation, and multimodal reasoning.

References

- [1] J. Achiam, S. Adler, S. Agarwal, L. Ahmad, I. Akkaya, F. L. Aleman, D. Almeida, J. Altenschmidt, S. Altman, S. Anadkat, et al. Gpt-4 technical report. *arXiv preprint arXiv:2303.08774*, 2023.
- [2] Anthropic. The claude 3 model family: Opus, sonnet, haiku. .
- [3] Anthropic. Claude 3.5 sonnet. .
- [4] S. Bai, K. Chen, X. Liu, J. Wang, W. Ge, S. Song, K. Dang, P. Wang, S. Wang, J. Tang, H. Zhong, Y. Zhu, M. Yang, Z. Li, J. Wan, P. Wang, W. Ding, Z. Fu, Y. Xu, J. Ye, X. Zhang, T. Xie, Z. Cheng, H. Zhang, Z. Yang, H. Xu, and J. Lin. Qwen2.5-vl technical report. *arXiv preprint arXiv:2502.13923*, 2025.
- [5] Y. Bai, A. Jones, K. Ndousse, A. Askell, A. Chen, N. DasSarma, D. Drain, S. Fort, D. Ganguli, T. Henighan, et al. Training a helpful and harmless assistant with reinforcement learning from human feedback. *arXiv preprint arXiv:2204.05862*, 2022.
- [6] Y. Bai, S. Kadavath, S. Kundu, A. Askell, J. Kernion, A. Jones, A. Chen, A. Goldie, A. Mirhoseini, C. McKinnon, et al. Constitutional ai: Harmlessness from ai feedback. *arXiv preprint arXiv:2212.08073*, 2022.
- [7] G. Brazil, A. Kumar, J. Straub, N. Ravi, J. Johnson, and G. Gkioxari. Omni3D: A large benchmark and model for 3D object detection in the wild. In *CVPR*, Vancouver, Canada, June 2023. IEEE.
- [8] W. Cai, Y. Ponomarenko, J. Yuan, X. Li, W. Yang, H. Dong, and B. Zhao. Spatialbot: Precise spatial understanding with vision language models. *arXiv preprint arXiv:2406.13642*, 2024.

- [9] B. Chen, Z. Xu, S. Kirmani, B. Ichter, D. Sadigh, L. Guibas, and F. Xia. Spatialvlm: Endowing vision-language models with spatial reasoning capabilities. In *Proceedings of the IEEE/CVF Conference on Computer Vision and Pattern Recognition*, pages 14455–14465, 2024.
- [10] A.-C. Cheng, Y. Ji, Z. Yang, Z. Gongye, X. Zou, J. Kautz, E. Bıyık, H. Yin, S. Liu, and X. Wang. Navila: Legged robot vision-language-action model for navigation. *arXiv preprint arXiv:2412.04453*, 2024.
- [11] A.-C. Cheng, H. Yin, Y. Fu, Q. Guo, R. Yang, J. Kautz, X. Wang, and S. Liu. Spatialrgpt: Grounded spatial reasoning in vision language models. *arXiv preprint arXiv:2406.01584*, 2024.
- [12] T. Chu, Y. Zhai, J. Yang, S. Tong, S. Xie, D. Schuurmans, Q. V. Le, S. Levine, and Y. Ma. Sft memorizes, rl generalizes: A comparative study of foundation model post-training. *arXiv preprint arXiv:2501.17161*, 2025.
- [13] R. Coulom. Efficient selectivity and backup operators in monte-carlo tree search. In *International conference on computers and games*, pages 72–83. Springer, 2006.
- [14] J. Gao, B. Sarkar, F. Xia, T. Xiao, J. Wu, B. Ichter, A. Majumdar, and D. Sadigh. Physically grounded vision-language models for robotic manipulation. In *IEEE International Conference on Robotics and Automation (ICRA)*. IEEE, 2024.
- [15] Google. Introducing gemini 2.0: our new ai model for the agentic era, 2024. URL <https://blog.google/technology/google-deepmind/google-gemini-ai-update-december-2024>. Accessed: Dec 2024.
- [16] A. Graves. Sequence transduction with recurrent neural networks. *arXiv preprint arXiv:1211.3711*, 2012.
- [17] D. Guo, D. Yang, H. Zhang, J. Song, R. Zhang, R. Xu, Q. Zhu, S. Ma, P. Wang, X. Bi, et al. Deepseek-r1: Incentivizing reasoning capability in llms via reinforcement learning. *arXiv preprint arXiv:2501.12948*, 2025.
- [18] W. Huang, C. Wang, Y. Li, R. Zhang, and L. Fei-Fei. Rekep: Spatio-temporal reasoning of relational keypoint constraints for robotic manipulation. *arXiv preprint arXiv:2409.01652*, 2024.
- [19] D. A. Hudson and C. D. Manning. Gqa: A new dataset for real-world visual reasoning and compositional question answering. In *Proceedings of the IEEE/CVF conference on computer vision and pattern recognition*, pages 6700–6709, 2019.
- [20] J. Johnson, B. Hariharan, L. Van Der Maaten, L. Fei-Fei, C. Lawrence Zitnick, and R. Girshick. Clevr: A diagnostic dataset for compositional language and elementary visual reasoning. In *Proceedings of the IEEE conference on computer vision and pattern recognition*, pages 2901–2910, 2017.
- [21] K. Kumar, T. Ashraf, O. Thawakar, R. M. Anwer, H. Cholakkal, M. Shah, M.-H. Yang, P. H. Torr, F. S. Khan, and S. Khan. Llm post-training: A deep dive into reasoning large language models. *arXiv preprint arXiv:2502.21321*, 2025.
- [22] A. Kuznetsova, H. Rom, N. Alldrin, J. Uijlings, I. Krasin, J. Pont-Tuset, S. Kamali, S. Popov, M. Mallocci, A. Kolesnikov, T. Duerig, and V. Ferrari. The open images dataset v4: Unified image classification, object detection, and visual relationship detection at scale. *IJCV*, 2020.

- [23] W. Kwon, Z. Li, S. Zhuang, Y. Sheng, L. Zheng, C. H. Yu, J. E. Gonzalez, H. Zhang, and I. Stoica. Efficient memory management for large language model serving with pagedattention. In *Proceedings of the ACM SIGOPS 29th Symposium on Operating Systems Principles*, 2023.
- [24] Z. Li, X. Wang, E. Stengel-Eskin, A. Kortylewski, W. Ma, B. Van Durme, and A. L. Yuille. Superclevr: A virtual benchmark to diagnose domain robustness in visual reasoning. In *Proceedings of the IEEE/CVF conference on computer vision and pattern recognition*, pages 14963–14973, 2023.
- [25] H. Liu, C. Li, Q. Wu, and Y. J. Lee. Visual instruction tuning. *Advances in neural information processing systems*, 36:34892–34916, 2023.
- [26] H. Liu, C. Li, Y. Li, and Y. J. Lee. Improved baselines with visual instruction tuning. In *Proceedings of the IEEE/CVF Conference on Computer Vision and Pattern Recognition*, pages 26296–26306, 2024.
- [27] Y. Liu, H. Duan, Y. Zhang, B. Li, S. Zhang, W. Zhao, Y. Yuan, J. Wang, C. He, Z. Liu, et al. Mmbench: Is your multi-modal model an all-around player? In *European conference on computer vision*, pages 216–233. Springer, 2024.
- [28] Z. Liu, C. Chen, W. Li, P. Qi, T. Pang, C. Du, W. S. Lee, and M. Lin. Understanding r1-zero-like training: A critical perspective. *arXiv preprint arXiv:2503.20783*, 2025.
- [29] B. P. Lowerre and B. R. Reddy. Harpy, a connected speech recognition system. *The Journal of the Acoustical Society of America*, 59(S1):S97–S97, 1976.
- [30] W. Ma, A. Wang, A. Yuille, and A. Kortylewski. Robust category-level 6d pose estimation with coarse-to-fine rendering of neural features. In *European Conference on Computer Vision*, pages 492–508. Springer, 2022.
- [31] W. Ma, H. Chen, G. Zhang, C. M. de Melo, A. Yuille, and J. Chen. 3dsrbench: A comprehensive 3d spatial reasoning benchmark. *arXiv preprint arXiv:2412.07825*, 2024.
- [32] W. Ma, G. Zhang, Q. Liu, G. Zeng, A. Kortylewski, Y. Liu, and A. Yuille. Imagenet3d: Towards general-purpose object-level 3d understanding. *Advances in Neural Information Processing Systems*, 37:96127–96149, 2024.
- [33] W. Ma, L. Ye, C. M. de Melo, A. Yuille, and J. Chen. Spatialllm: A compound 3d-informed design towards spatially-intelligent large multimodal models. In *Proceedings of the IEEE/CVF Conference on Computer Vision and Pattern Recognition*, pages 26296–26306, 2025.
- [34] J. Mao, C. Gan, P. Kohli, J. B. Tenenbaum, and J. Wu. The Neuro-Symbolic Concept Learner: Interpreting Scenes, Words, and Sentences From Natural Supervision. In *International Conference on Learning Representations*, 2019. URL <https://openreview.net/forum?id=rJgMlhRctm>.
- [35] N. Muennighoff, Z. Yang, W. Shi, X. L. Li, L. Fei-Fei, H. Hajishirzi, L. Zettlemoyer, P. Liang, E. Candès, and T. Hashimoto. s1: Simple test-time scaling. *arXiv preprint arXiv:2501.19393*, 2025.
- [36] OpenAI. Introducing openai o3 and o4-mini, 2025. URL <https://openai.com/index/introducing-o3-and-o4-mini/>. Accessed: Apr 2025.
- [37] R. Rafailov, A. Sharma, E. Mitchell, C. D. Manning, S. Ermon, and C. Finn. Direct preference optimization: Your language model is secretly a reward model. *Advances in Neural Information Processing Systems*, 36:53728–53741, 2023.

- [38] N. Ravi, V. Gabeur, Y.-T. Hu, R. Hu, C. Ryali, T. Ma, H. Khedr, R. Rädle, C. Rolland, L. Gustafson, et al. Sam 2: Segment anything in images and videos. *arXiv preprint arXiv:2408.00714*, 2024.
- [39] A. Ray, J. Duan, R. Tan, D. Bashkirova, R. Hendrix, K. Ehsani, A. Kembhavi, B. A. Plummer, R. Krishna, K.-H. Zeng, et al. Sat: Spatial aptitude training for multimodal language models. *arXiv preprint arXiv:2412.07755*, 2024.
- [40] remyxai. Remyxai/spacellava, 2024. URL <https://huggingface.co/remyxai/SpaceLLaVA>.
- [41] Z. Shao, P. Wang, Q. Zhu, R. Xu, J. Song, X. Bi, H. Zhang, M. Zhang, Y. Li, Y. Wu, et al. Deepseekmath: Pushing the limits of mathematical reasoning in open language models. *arXiv preprint arXiv:2402.03300*, 2024.
- [42] C. Snell, J. Lee, K. Xu, and A. Kumar. Scaling llm test-time compute optimally can be more effective than scaling model parameters. *arXiv preprint arXiv:2408.03314*, 2024.
- [43] H. Sun, M. Haider, R. Zhang, H. Yang, J. Qiu, M. Yin, M. Wang, P. Bartlett, and A. Zanette. Fast best-of-n decoding via speculative rejection. *arXiv preprint arXiv:2410.20290*, 2024.
- [44] G. R. Team, S. Abeyruwan, J. Ainslie, J.-B. Alayrac, M. G. Arenas, T. Armstrong, A. Balakrishna, R. Baruch, M. Bauza, M. Blokzijl, et al. Gemini robotics: Bringing ai into the physical world. *arXiv preprint arXiv:2503.20020*, 2025.
- [45] G. Tie, Z. Zhao, D. Song, F. Wei, R. Zhou, Y. Dai, W. Yin, Z. Yang, J. Yan, Y. Su, et al. A survey on post-training of large language models. *arXiv preprint arXiv:2503.06072*, 2025.
- [46] P. Tong, E. Brown, P. Wu, S. Woo, A. J. V. IYER, S. C. Akula, S. Yang, J. Yang, M. Middepogu, Z. Wang, et al. Cambrian-1: A fully open, vision-centric exploration of multimodal llms. *Advances in Neural Information Processing Systems*, 37:87310–87356, 2024.
- [47] X. Wang, W. Ma, Z. Li, A. Kortylewski, and A. L. Yuille. 3d-aware visual question answering about parts, poses and occlusions. *Advances in Neural Information Processing Systems*, 36: 58717–58735, 2023.
- [48] X. Wang, W. Ma, A. Wang, S. Chen, A. Kortylewski, and A. Yuille. Compositional 4d dynamic scenes understanding with physics priors for video question answering. *arXiv preprint arXiv:2406.00622*, 2024.
- [49] X. Wang, W. Ma, T. Zhang, C. M. de Melo, J. Chen, and A. Yuille. Pulsecheck457: A diagnostic benchmark for comprehensive spatial reasoning of large multimodal models. *arXiv preprint arXiv:2502.08636*, 2025.
- [50] J. Wei, M. Bosma, V. Y. Zhao, K. Guu, A. W. Yu, B. Lester, N. Du, A. M. Dai, and Q. V. Le. Finetuned language models are zero-shot learners. *arXiv preprint arXiv:2109.01652*, 2021.
- [51] J. Wei, X. Wang, D. Schuurmans, M. Bosma, F. Xia, E. Chi, Q. V. Le, D. Zhou, et al. Chain-of-thought prompting elicits reasoning in large language models. *Advances in neural information processing systems*, 35:24824–24837, 2022.
- [52] J. Yang, S. Yang, A. W. Gupta, R. Han, L. Fei-Fei, and S. Xie. Thinking in space: How multimodal large language models see, remember, and recall spaces. *arXiv preprint arXiv:2412.14171*, 2024.

- [53] L. Yang, B. Kang, Z. Huang, Z. Zhao, X. Xu, J. Feng, and H. Zhao. Depth anything v2. *Advances in Neural Information Processing Systems*, 37:21875–21911, 2024.
- [54] S. Yao, D. Yu, J. Zhao, I. Shafran, T. Griffiths, Y. Cao, and K. Narasimhan. Tree of thoughts: Deliberate problem solving with large language models. *Advances in neural information processing systems*, 36:11809–11822, 2023.
- [55] C. Zhou, P. Liu, P. Xu, S. Iyer, J. Sun, Y. Mao, X. Ma, A. Efrat, P. Yu, L. Yu, et al. Lima: Less is more for alignment. *Advances in Neural Information Processing Systems*, 36:55006–55021, 2023.

Appendix

A. Implementation detail

We train SpatialReasoner using different combinations of curated datasets and training objectives. Starting from the Qwen2.5-VL-7B [4] base model, we first apply SFT with 24k curated SR-CoT data alongside 24k randomly sampled LLaVA [25] data, resulting in SpatialReasoner-SFT. Next, we further train SpatialReasoner-SFT with RL using 1.2k SR-QA examples, leading to our final SpatialReasoner. For comparison, if we instead fine-tune SpatialReasoner-SFT with SFT on the same 1.2k SR-QA set, we obtain SpatialReasoner-SFT (+HQ SFT), serving as an ablation study baseline. In parallel, we directly fine-tune the base model with RL using only the 1.2k SR-QA data without prior SFT, resulting in SpatialReasoner-Zero. Additionally, to investigate whether explicit 3D perception capabilities can enable the model to self-organize reasoning trajectories under process rewards, we train the base model with SFT using 12k Basic3D-QA data alongside 12k randomly sampled LLaVA data before applying RL training on the 1.2k SR-QA data, yielding SpatialReasoner-Zero (w/ 3D Rwd).

We conduct all training experiments using 4×NVIDIA H100 80GB HBM3 GPUs. For SFT, we train the model for 10 epochs (approximately 20K steps with a batch size of 6) on the combined 24k SR-CoT and 24k LLaVA datasets. For RL training, we train for 100 epochs (approximately 13K steps with a batch size of 12) on the 1.2k SR-QA dataset, using 1 GPU with vLLM [23] for efficient inference acceleration. For the experiments withholding multi-object training examples, we double the number of training epochs to compensate for the reduced training set size. We set the learning rate to 5e-6 for SFT and 5e-7 for RL, both following a cosine learning rate scheduler with a warm-up ratio of 0.1. In the KL divergence ablation study, we set the KL penalty weight to 0.04. We monitored the model every 1K training steps and reported results based on the best-performing checkpoint.

B. 2D Reasoning as a Shortcut

As shown in Table 1 and Table 2, our SpatialReasoner outperforms previous open-source and proprietary models on 3DSRBench [31], and achieves notable improvements on GQA [19] (from 58.8% to 61.8%) and depth-related questions in CVBench-3D [46] (from 82.5% to 87.3%). However, if we focus specifically on multi-object 3D distance-related questions in CVBench-3D [46] and 3DSRBench [31], we observe contradictory results: SpatialReasoner achieves a substantial improvement of 21.5% on 3DSRBench, but exhibits a notable performance drop of 9.9% on CVBench-3D (see Table 7).

We attribute this discrepancy to the abundant shortcuts in distance-related questions in CVBench-3D. From the qualitative examples in Figure 9, the provided 2D bounding boxes in CVBench-3D can be exploited as shortcuts to answer the 3D spatial reasoning question. Rather than reasoning about 3D distances between objects, we can easily derive the correct answer by comparing the 2D distances between the red and blue boxes and between the red and green boxes. Meanwhile, 3DSRBench is a human-collected VQA dataset and manually avoid such spurious correlation, e.g., “objects closer in 3D space are also closer in 2D image plane”. For the 3DSRBench example in Figure 9, the bounding box of the dog is actually closer to the bounding box of the man in black than farther away in 3D space.

Given the 2D bounding box annotations in CVBench-3D and 3DSRBench, we derive a simple heuristic that attempts to answer distance-related spatial reasoning questions by simply comparing L2 distances between 2D centers of the object bounding boxes. We achieve a 80.2% accuracy on distance questions in CVBench-3D and 34.3% in 3DSRBench. **This demonstrates that baseline models such as Qwen2.5-VL are largely exploiting 2D spatial reasoning as a shortcut to answer complex 3D spatial reasoning questions.** Meanwhile, with our 3D-aware post-training, our SpatialReasoner

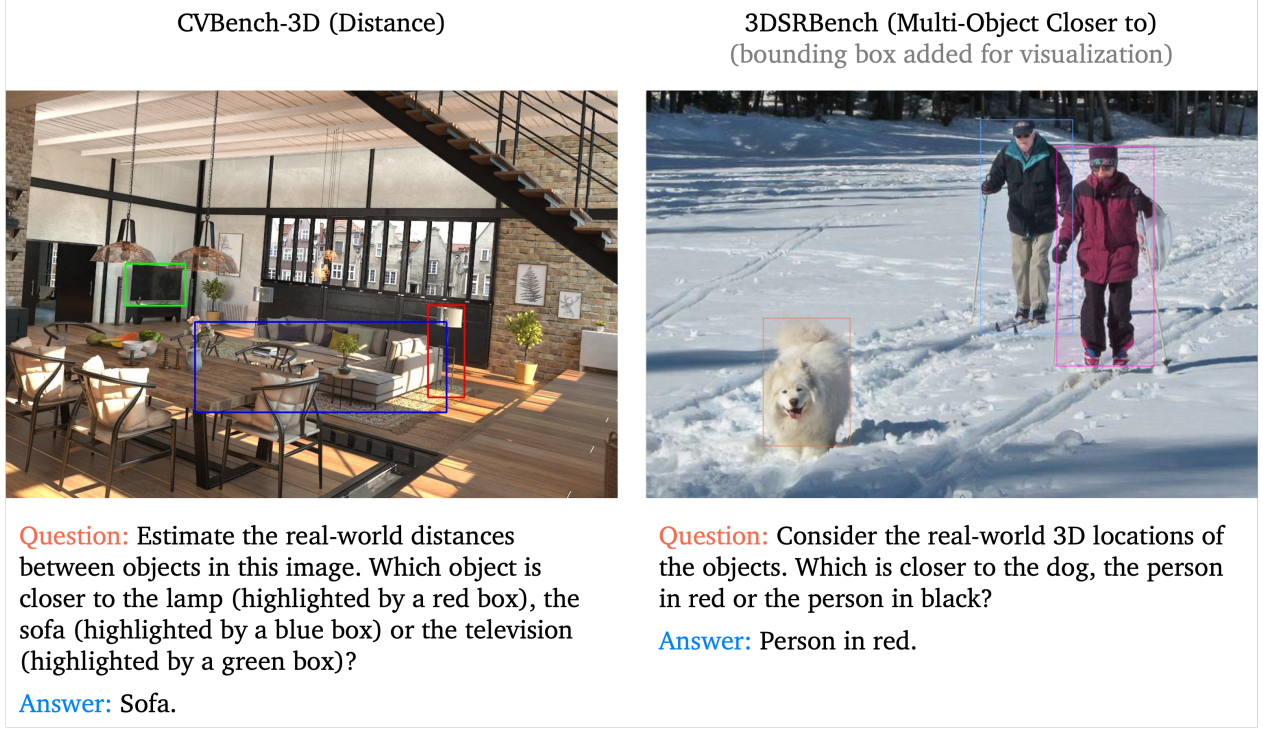


Figure 9 | Comparison between (multi-object) distance-related questions in CVBench-3D [46] and 3DSRBench [31].

Method	CVBench3D Distance	3DSRBench multi-object-closer-to
2D Heuristic	80.2	34.3
Qwen2.5-VL-7B-Instruct [4]	83.2	49.4
SpatialReasoner	73.3	70.9

Table 7 | Comparison between Qwen2.5-VL [4] and SpatialReasoner on (multi-object) 3D distance-related questions in CVBench-3D [46] and 3DSRBench [31].

adopts explicit 3D representation for various 3D spatial reasoning questions. **The trade-off between exploiting 2D shortcuts and adopting explicit 3D representations results in slightly lower performance of SpatialReasoner on test data with abundant spurious correlations, but more importantly, leads to a robust and largely improved performance on a challenging real-world datasets.**

💡 **Visual cues or explicit 3D reasoning?** LVLMs that exploit 2D reasoning as shortcuts may achieve improved performance on test data with abundant spurious correlations (e.g., distance questions in CVBench-3D). However, they cannot genuinely solve 3D spatial reasoning problems and fall far behind SpatialReasoner that builds on explicit 3D spatial reasoning when tested on challenging real-world problems in 3DSRBench.